Spin Crossover

Deutsche Ausgabe: DOI: 10.1002/ange.201500288
Internationale Ausgabe: DOI: 10.1002/anie.201500288

Fe^{II} Spin-Crossover Phenomenon in the Pentadecanuclear $\{Fe_9[Re(CN)_8]_6\}$ Spherical Cluster**

Szymon Chorazy, Robert Podgajny, Koji Nakabayashi, Jan Stanek, Michał Rams, Barbara Sieklucka, and Shin-ichi Ohkoshi**

Abstract: *The self-assembly of iron(II) ions with rare octacyanidorhenate(V) metalloligands in a methanolic solution results in the formation of a nanometric pentadecanuclear $\{Fe^{II}_9[Re^{V}(CN)_8]_6(MeOH)_{24}\}\cdot 10\,MeOH$ (**1**) molecule with a six-capped body-centered cubic topology. The cluster demonstrates a thermally-induced spin-crossover phase transition at $T_{1/2} = 195$ K which occurs selectively for a single Fe^{II} ion embedded in the center of a cluster core.*

Molecule-based magnets, built of magnetically active metal complexes or organic radicals, have been intensively studied because of various magnetic properties, including magnetic ordering below the critical temperature (T_c),[1–3] spin-transition phenomena,[4–6] and slow magnetic relaxation.[7–9] Significant interest has been focused on cyanido-bridged bimetallic assemblies which exhibit magnetic coupling of a predictable strength, giving magnetic ordering at various T_c values, in some cases up to 100 °C.[10–12] These systems were found to efficiently combine magnetism with other functionalities, such as ferroelectricity,[13] chirality,[14–17] luminescence,[18] sensitivity to guest molecules,[19–21] zero thermal expansion,[22] or photoinduced phase transitions.[24–26] The interaction between this additional property and magnetism gives rise to extra cross-effects.[27–30] We have shown magnetic second harmonic generation (MSHG),[31,32] light-induced spin-crossover magnetism,[23] and a 90° switching of the SHG polarization plane when chirality was coupled with photomagnetism.[14]

Magnetic materials based on polynuclear clusters have attracted particular attention as they can show a high-spin ground state leading to single-molecule magnetism (SMM)[33] or to a magnetocaloric effect.[34] Among such materials, bimetallic $[M(CN)_8]$-based clusters have great potential,[35] as demonstrated by a family of $\{M_9M'_6\}$ pentadecanuclear clusters $\{M^{II}_9[M'^{V}(CN)_8]_6(MeOH)_{24}\}$ (M = 3d metal; M′ = Mo, W; MeOH = methanol) which show a diverse range of magnetic functionalities, including high spin,[36–38] SMM,[39,40] and thermally induced charge transfer.[41,42]

In this regard, the application of the spin-crossover (SCO) effect to polynuclear molecules is rare. SCO was broadly investigated for mononuclear complexes, based mainly on the Fe^{II} ion,[43,44] and coordination polymers offering efficient intramolecular interactions giving thermal hysteresis loops, crucial for applications such as memory devices.[45,46] Apart from a number of di- and tetranuclear species which demonstrate a spectacular multistep SCO effect,[47–50] there are only three well-characterized examples of larger SCO clusters: a) pentanuclear $\{[Fe^{II}(tmphen)_2]_3[M^{III}(CN)_6]_2\}$ (tmphen = 3,4,7,8-tetramethyl-1,10-phenanthroline; M = Fe, Co),[51] b) heptanuclear $\{[Fe^{III}(salpet)]_6[Fe^{II}(CN)_6]\}Cl_2$ (salpet = a pendadentate Schiff base),[52] and c) tetradecanuclear $\{Fe^{II}_6[Cu^{I}(Tp^{4-py})]_8\}^{4+}$ ($Tp^{4\text{-}py}$ = tris{3-(4-pyridyl)-pyrazol-1-yl}hydroborate).[53] Other SCO clusters of Fe^{III} ions with cyanidometallates, built of five to twelve centers, were characterized only by ^{57}Fe Mössbauer spectroscopy.[54,55] Thus, we focused our effort on the preparation of large SCO clusters which can be promising for both multistep SCO and cluster-based coordination polymers. Continuing our interest in CN^--bridged $\{M_9M'_6\}$ clusters, we aimed to introduce SCO Fe^{II} ions into this structure. Our previous attempt with $[W^{V}(CN)_8]^{3-}$ resulted in the formation of $\{Fe_9W_6\}$ molecule showing an iron(II)–tungsten(V) to iron(III)–tungsten(IV) charge-transfer (CT) process instead of an SCO effect.[41] We next used a rare $[Re^{V}(CN)_8]^{3-}$ molecule which was reported by J. R. Long et al.[56,57] as a product of thermal decomposition

[*] Dr. S. Chorazy, Dr. K. Nakabayashi, Prof. Dr. S. Ohkoshi
Department of Chemistry, School of Science
The University of Tokyo, 7-3-1 Hongo
Bunkyo-ku, Tokyo113-0033 (Japan)
E-mail: szymon@chem.s.u-tokyo.ac.jp
ohkoshi@chem.s.u-tokyo.ac.jp
Homepage: Homepage: http://www.chem.s.u-tokyo.ac.jp/users/ssphys/english/
Dr. S. Chorazy, Dr. R. Podgajny, Prof. Dr. B. Sieklucka
Faculty of Chemistry, Jagiellonian University
Ingardena 3, 30-060 Kraków (Poland)
Prof. Dr. J. Stanek, Dr. M. Rams
Institute of Physics, Jagiellonian University
Łojasiewicza 11, 30-348 Kraków (Poland)
Prof. Dr. S. Ohkoshi
CREST, JST, K's Gobancho
7 Gobancho, Chiyoda-ku, Tokyo 102-0076 (Japan)

[**] We thank the Core Research for Evolutional Science and Technology (CREST) program of the Japan Science and Technology Agency (JST), the Advanced Photon Science Alliance from the Ministry of Education, Culture, Sports, Science, and Technology of Japan (MEXT), the Global Science course from MEXT, the Cryogenic Research Center, the Center for Nano Lithography and Analysis, and the University of Tokyo. S.C. acknowledges the support of the Foundation for Polish Science within a START fellowship 2014 and the Polish Ministry of Science and Higher Education within the Iuventus Plus program (IP2014 006073).

Supporting information for this article (including experimental details, crystallographic data, additional structural views, and plots of magnetic properties) is available on the WWW under http://dx.doi.org/10.1002/anie.201500288.

of $[Re^{IV}(CN)_7]^{4-}$ in the presence of KIO_4 and $MnCl_2$. Its voltammetry suggested that $[Re^{V}(CN)_8]^{3-}$ has an accessible Re^{VI} instead of a Re^{IV} oxidation state.[56] Thus, it should stabilize the Fe^{II} state, providing an opportunity to potentially detect the SCO effect on a 3d metal center. Following this procedure, we report the structure and properties of a $\{Fe^{II}_9[Re^{V}(CN)_8]_6(MeOH)_{24}\}\cdot 10\,MeOH$ (**1**) cluster showing an Fe^{II} spin-crossover effect, demonstrated by temperature-dependent structural, spectroscopic, and magnetic studies.

Yellow crystals of **1** were obtained by the self-assembly of Fe^{II} chloride with an organic salt of $[Re^{V}(CN)_8]^{3-}$ in methanol (see Figure S1 in the Supporting Information and details therein). Single-crystal X-ray diffraction was performed at 240(2) and 120(2) K.[60] The related high- and low-temperature phases are denoted $\mathbf{1}^{HT}$ and $\mathbf{1}^{LT}$, respectively. $\{Fe^{II}_9[Re^{V}(CN)_8]_6(MeOH)_{24}\}$ (**1**) consists of CN^--bridged $\{Fe_9Re_6\}$ clusters of a six-capped body-centered cubic topology, analogous to other members of the $\{M^{II}_9[M'^{V}(CN)_8]_6(MeOH)_{24}\}$ family (M = 3d metal, M′ = Mo, W; see Figure 1 and Table 1 and Figures S2–S3 and Tables S1–S3 in the Supporting Information).[36–42] This molecule comprises one $[Fe^{II}(NC)_6]^{4-}$ complex (containing atom Fe1) located in the center of a cube, where corners are occupied by eight $[Fe^{II}(MeOH)_3(NC)_3]^-$ ions, involving four crystallographically unique Fe sites (Fe2–Fe5). Six $[Re^{V}(CN)_8]^{3-}$ units cap the faces of the Fe-based cube which completes the almost spherical cluster (Figure 1).

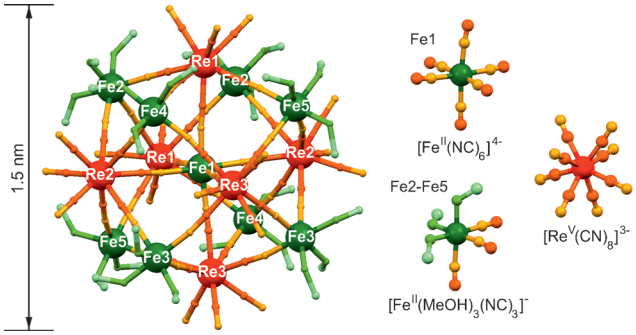

Figure 1. The structure of the cluster $\{Fe^{II}_9[Re^{V}(CN)_8]_6(MeOH)_{24}\}$ (**1**) and detailed views of the coordination geometry of the Fe^{II} and Re^{V} complexes embedded in the cluster core.

The average Fe–N/O bond lengths at high ($\mathbf{1}^{HT}$) and low temperature ($\mathbf{1}^{LT}$) are given in Table 1. In $\mathbf{1}^{HT}$, the average Fe–N distance for Fe1 is close to 2.06 Å, whereas for the Fe2–Fe5 centers the mean lengths of Fe–N/O bonds are in the range 2.13–2.14 Å. These lengths are in good agreement with values measured in octahedral high-spin Fe^{II} centers ($^{HS}Fe^{II}$) in CN^--bridged systems.[14,41] In $\mathbf{1}^{LT}$, the Fe–N/O distances for Fe2–Fe5 atoms decrease gradually because of a standard thermal contraction. On the contrary, the Fe1–N bond lengths change by approximately 6% to give a mean value of 1.93 Å which can be assigned to a low-spin Fe^{II} center ($^{LS}Fe^{II}$).[4,14] This suggests that **1** demonstrates the spin-crossover effect selectively for internal Fe1 centers whereas the external Fe2–Fe5 sites remain in the high-spin state because of differences in their coordination spheres. Fe1 coordinates six CN^- ligands through the N atoms, which gives an intermediate ligand-field strength suitable in magnitude for the SCO effect to occur, as shown for Prussian Blue analogues.[58] Fe2–Fe5 sites have a mixed N_3O_3 coordination geometry, resulting in insufficient ligand-field strength for the SCO effect to occur.[58]

Table 1: Average Fe–N/O bond lengths [Å] for **1**.

T/K	Fe1	Fe2	Fe3	Fe4	Fe5
240(2), $\mathbf{1}^{HT}$	2.06(1)	2.13(1)	2.14(1)	2.14(1)	2.13(1)
120(2), $\mathbf{1}^{LT}$	1.93(1)	2.12(1)	2.13(2)	2.13(2)	2.12(1)

The structural transition on Fe1 sites implies changes in other metric parameters of the cluster (Table S2). On cooling from $\mathbf{1}^{HT}$ to $\mathbf{1}^{LT}$, the mean Fe1–Re distance is decreased by circa 1.5%, whereas smaller decreases of 0.4% are found for other Fe–Re bridges. All Re–C bond lengths remain unchanged, and the dodecahedral geometry of $[Re^{V}(CN)_8]^{3-}$ is preserved (Table S3). It suggests that the Re^{V} state is stable during the transition, and the cyanide complex serves only as a flexible mediator in the propagation of the SCO effect. The structural transition in a cluster is accompanied by the shortening of intercluster $Fe{-}O_{MeOH}\cdots NC{-}W$ hydrogen bonds, and the expected unit-cell compression from 16236.2(7) to 15675.7(15) $Å^3$ ($\approx$3.5%) is detected (Figure S3).

On cooling from $\mathbf{1}^{HT}$ to $\mathbf{1}^{LT}$, the color of the crystals changed from yellow to blue. This is connected with the appearance of a low-spin Fe^{II} center which gives rise to strong absorption of visible light as a result of their d–d transitions (Figure S1). The analysis of the Fe oxidation state in $\mathbf{1}^{HT}$ and $\mathbf{1}^{LT}$ was performed by ^{57}Fe Mössbauer spectroscopy (Figure 2). The spectrum at 295 K was deconvoluted into two doublets ascribed to high-spin Fe^{II} with isomer shifts of $\delta = 1.25(1)$ and 1.39(1) $mm\,s^{-1}$ (Table 2).[4] The broad line component is assigned to Fe2–Fe5 sites of four slightly different quadrupole splitting values. The inner doublet indicates the crystallographically different Fe1 site. This component transforms at 80 K into the doublet at $\delta = 0.46\ mm\,s^{-1}$ with a very small quadrupole splitting of $\Delta E_Q = 0.12\ mm\,s^{-1}$ which is attributable to the low-spin Fe^{II} center. The relative intensity of the signal attributable to the low-spin Fe^{II} is 8 ± 2% which agrees well with the structural studies showing that only one Fe center in the $\{Fe_9Re_6\}$ cluster exhibits the SCO effect. The remaining doublets attributable to the high-spin Fe^{II} center show the characteristic behavior for a $3d^6$ configuration, that is an increase in quadrupole splitting with decreasing temperature. Moreover, the Fe2–Fe5 states are divided into two groups characterized by two doublets with an intensity ratio of 1:3. This indicates that the ligand arrangement around one of these states, probably Fe2, is different, as suggested by structural studies (Table S3).

The SCO transition in **1** influences the magnetic properties of the cluster (see Figure 3 and Figures S4 and S5). The room-temperature product of magnetic susceptibility and temperature ($\chi_M T$) is 33.7 $cm^3\,mol^{-1}\,K$ for the $\{Fe_9Re_6\}$ unit which corresponds to nine uncoupled high-spin Fe^{II} centers ($S = 2$) separated by a diamagnetic $[Re^{V}(CN)_8]^{3-}$ unit.[56] The

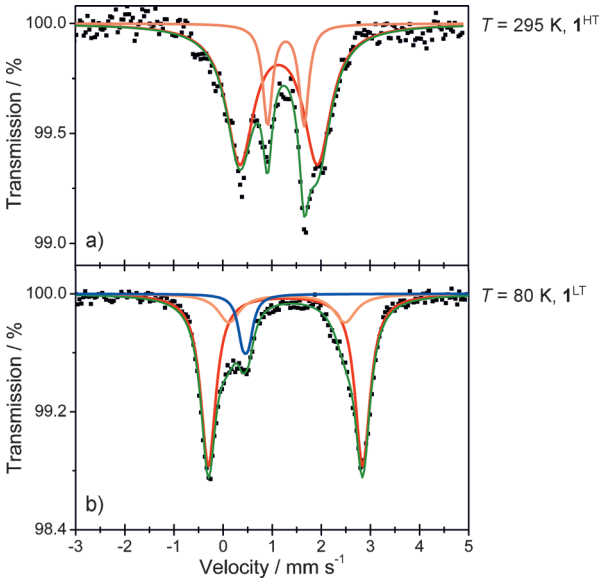

Figure 2. ^{57}Fe Mössbauer spectra of **1** at a) 295 K and at b) 80 K. Experimental results are shown as black data points. The fitted results are shown as solid lines. Colors: $^{LS}Fe^{II}$ (blue), $^{HS}Fe^{II}$ (red and orange), total calculated fit (green).

Table 2: ^{57}Fe Mössbauer spectral parameters for **1**.

T [K]	Fe site	δ [mm s^{-1}]	ΔE_Q [mm s^{-1}]	Area contribution [%]
295(1), **1**^{HT}	HS Fe^{II}	1.25(1)	1.58(2)	80(4)
	HS Fe^{II}	1.39(1)	0.74(2)	20(4)
80(1), **1**^{LT}	HS Fe^{II}	1.30(1)	3.14(2)	70(2)
	HS Fe^{II}	1.27(1)	2.36(2)	22(2)
	LS Fe^{II}	0.46(1)	0.12(2)	8(2)

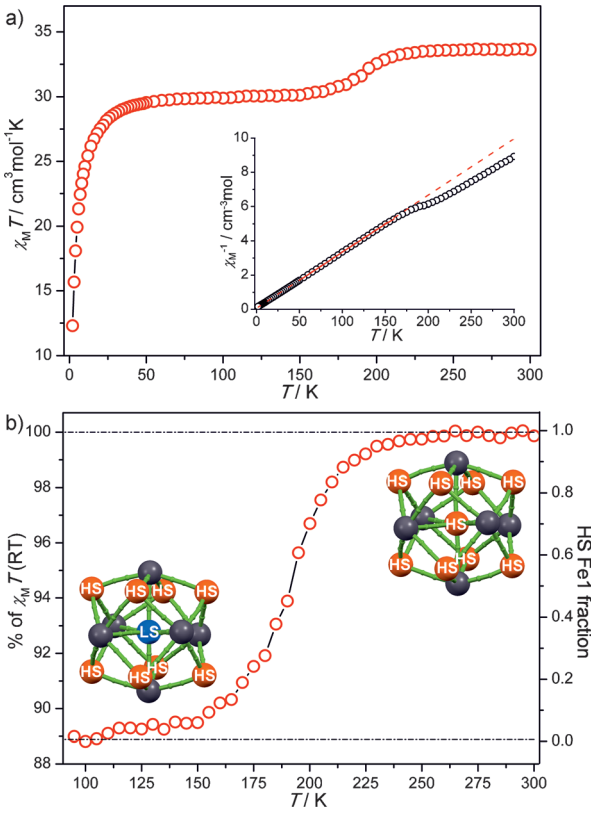

Figure 3. a) Plot of $\chi_M T$ values versus temperature (T) with the Curie–Weiss law fit (red line) for **1** (H_{dc} = 1000 Oe). Inset in (a): χ_M^{-1} values plotted against T. b) The related T dependence of the relative decrease in the $\chi_M T$ value compared with the room-temperature value (% of $\chi_M T$(RT)) which corresponds to the Fe1 HS fraction.

average g value of Fe^{II} is 2.23 which is in the 2.2–2.3 range, typical for CN$^-$-bridged systems with high-spin Fe^{II} centers.[14,41] On cooling, the $\chi_M T$ value remains unchanged to 220 K, later decreases strongly over the next 60 K, reaching 30.2 cm^3 mol^{-1} K at 160 K. On further cooling, the decrease is slow to 30 K, and much faster below this point (Figure 3). The first decrease of the $\chi_M T$ value can be assigned to the spin crossover resulting in the transition from high-spin Fe^{II} ($S = 2$) to low-spin Fe^{II} ($S = 0$). The signal at 160 K is 89.6 % of the room-temperature value, which is in good agreement with the approximate 11 % decrease expected for the SCO occurring on a single Fe of the cluster (specifically Fe1). Thus, the relative decrease of the $\chi_M T$ value in comparison to the room-temperature value shows the temperature dependence of the Fe1 high-spin fraction. On increasing the temperature, the plot corresponds to the cooling data, with no thermal hysteresis observed. Considering the decrease in $\chi_M T$ value in the 220–160 K range, the largest change occurs within 20 K (205–185 K), and the transition temperature, measured from the temperature dependence of the first derivative of $\chi_M T$, is $T_{1/2} = 195$ K (Figure S4). The magnetization at $T = 1.8$ K as a function of magnetic field is not saturated at 50 kOe and reaches 25.6 Nβ, which is lower than the 35.7 Nβ expected for eight isolated high-spin Fe^{II} centers (Figure S5). This result, together with the abrupt decrease of the $\chi_M T$ value below 20 K and a negative value of the Weiss constant $\theta = -1.8$ K (obtained from the Curie–Weiss law fit to data in the 50–160 K range), confirm the occurrence of antiferromagnetic interactions which presumably lead to a zero-spin cluster at very low temperatures.

In conclusion, we have prepared a fifteen-metal-centered cyanido-bridged {Fe$^{II}_9$[Re^{V}(CN)$_8$]$_6$(MeOH)$_{24}$} (**1**) nanoball which is the highest nuclearity molecule reported exhibiting the spin-crossover effect.[4] **1** exhibits a $^{HS}Fe^{II} \leftrightarrow {}^{LS}Fe^{II}$ spin transition at $T_{1/2} = 195$ K which is induced selectively on a single Fe^{II} center embedded in a {Fe(NC)$_6$} unit in the center of a cluster. In contrast, the remaining eight Fe^{II} sites of the {Fe$_9$Re$_6$} cluster remain in the high-spin state because of mixed {FeN$_3$O$_3$} coordination. This selective spin-crossover effect was achieved by rational design based on our previous results with the analogous {Fe$_9$W$_6$} and {Fe$_6$Co$_3$W$_6$} clusters.[41,42] Our molecule potentially opens the way for a new class of SCO polynuclear systems. The challenge now is to induce the SCO effect on external Fe sites of a cluster core, which may be achieved by the coordination of appropriate N-donor ligands to replace labile, coordinated solvent molecules, as was reported for other members of the family of {M$_9$M′$_6$} clusters.[35,59] Alternatively, it should be possible to control the spin state of Fe sites using pressure or light irradiation.[14] Further studies along this line are in progress.

Keywords: cluster compounds · cyanide ligands · iron · rhenium · spin crossover

How to cite: *Angew. Chem. Int. Ed.* **2015**, *54*, 5093 – 5097
Angew. Chem. **2015**, *127*, 5182 – 5186

[1] L. Norel, J.-B. Rota, L.-M. Chamoreau, G. Pilet, V. Robert, C. Train, *Angew. Chem. Int. Ed.* **2011**, *50*, 7128 – 7131; *Angew. Chem.* **2011**, *123*, 7266 – 7269.
[2] E. Coronado, C. Marti-Gastaldo, J. R. Galan-Mascaros, M. Cavallini, *J. Am. Chem. Soc.* **2010**, *132*, 5456 – 5468.
[3] J. S. Miller, *Chem. Soc. Rev.* **2011**, *40*, 3266 – 3296.
[4] *Spin-Crossover Materials: Properties and Applications* (Ed.: M. A. Halcrow), Wiley, Oxford, **2013**.
[5] D. Papanikolaou, S. Margadonna, W. Kosaka, S. Ohkoshi, M. Brunelli, K. Prassides, *J. Am. Chem. Soc.* **2006**, *128*, 8358 – 8363.
[6] D. M. Pajerowski, J. E. Gardner, D. R. Talham, M. W. Meisel, *J. Am. Chem. Soc.* **2009**, *131*, 12927 – 12936.
[7] D. Gatteschi, R. Sessoli, J. Villain, *Molecular Nanomagnets, Mesoscopic Physics and Nanotechnology*, Oxford University Press, Oxford, **2006**.
[8] R. Bagai, G. Christou, *Chem. Soc. Rev.* **2009**, *38*, 1011 – 1026.
[9] V. Mougel, L. Chatelain, J. Pécaut, R. Caciuffo, E. Colineau, J.-C. Griveau, M. Mazzanti, *Nat. Chem.* **2012**, *4*, 1011 – 1017.
[10] S. Ferlay, T. Mallah, R. Ouahes, P. Veillet, M. Verdaguer, *Nature* **1995**, *378*, 701 – 703.
[11] S. M. Holmes, G. S. Girolami, *J. Am. Chem. Soc.* **1999**, *121*, 5593 – 5594.
[12] Ø. Hatlevik, W. E. Buschmann, J. Zhang, J. L. Manson, J. S. Miller, *Adv. Mater.* **1999**, *11*, 914 – 918.
[13] S. Ohkoshi, H. Tokoro, T. Matsuda, H. Takahashi, H. Irie, K. Hashimoto, *Angew. Chem. Int. Ed.* **2007**, *46*, 3238 – 3241; *Angew. Chem.* **2007**, *119*, 3302 – 3305.
[14] S. Ohkoshi, S. Takano, K. Imoto, M. Yoshikiyo, A. Namai, H. Tokoro, *Nat. Photonics* **2014**, *8*, 65 – 71.
[15] S. Chorazy, K. Nakabayashi, K. Imoto, J. Mlynarski, B. Sieklucka, S. Ohkoshi, *J. Am. Chem. Soc.* **2012**, *134*, 16151 – 16154.
[16] K. Inoue, K. Kikuchi, M. Ohba, H. Okawa, *Angew. Chem. Int. Ed.* **2003**, *42*, 4810 – 4813; *Angew. Chem.* **2003**, *115*, 4958 – 4961.
[17] S. Chorazy, R. Podgajny, W. Nitek, T. Fic, E. Görlich, M. Rams, B. Sieklucka, *Chem. Commun.* **2013**, *49*, 6731 – 6733.
[18] S. Chorazy, K. Nakabayashi, S. Ohkoshi, B. Sieklucka, *Chem. Mater.* **2014**, *26*, 4072 – 4075.
[19] P. Dechambenoit, J. R. Long, *Chem. Soc. Rev.* **2011**, *40*, 3249 – 3265.
[20] S. Ohkoshi, K. Arai, Y. Sato, K. Hashimoto, *Nat. Mater.* **2004**, *3*, 857 – 861.
[21] W. Kaneko, M. Ohba, S. Kitagawa, *J. Am. Chem. Soc.* **2007**, *129*, 13706 – 13712.
[22] S. Margadonna, K. Prassides, A. N. Fitch, *J. Am. Chem. Soc.* **2004**, *126*, 15390 – 15391.
[23] S. Ohkoshi, K. Imoto, Y. Tsunobuchi, S. Takano, H. Tokoro, *Nat. Chem.* **2011**, *3*, 564 – 569.
[24] S. Ohkoshi, H. Tokoro, *Acc. Chem. Res.* **2012**, *45*, 1749 – 1758.
[25] E. S. Koumousi, I.-R. Jeon, Q. Gao, P. Dechambenoit, D. N. Woodruff, P. Merzeau, L. Buisson, X. Jia, D. Li, F. Volatron, C. Mathonière, R. Clérac, *J. Am. Chem. Soc.* **2014**, *136*, 15461 – 15464.
[26] O. N. Risset, P. A. Quintero, T. V. Brinzari, M. J. Andrus, M. W. Lufaso, M. W. Meisel, D. R. Talham, *J. Am. Chem. Soc.* **2014**, *136*, 15660 – 15569.
[27] C. Train, M. Gruselle, M. Verdaguer, *Chem. Soc. Rev.* **2011**, *40*, 3297 – 3312.
[28] C. Train, R. Gheorghe, V. Krstic, L.-M. Chamoreau, N. S. Ovanesyan, G. Rikken, M. Gruselle, M. Verdaguer, *Nat. Mater.* **2008**, *7*, 729 – 734.
[29] W. Eerenstein, N. D. Mathur, J. F. Scott, *Nature* **2011**, *469*, 21 – 29.
[30] E. Pardo, C. Train, H. Liu, L.-M. Chamoreau, B. Dhkil, H. Boubekeur, F. Lloret, K. Nakatani, H. Tokoro, S. Ohkoshi, M. Verdaguer, *Angew. Chem. Int. Ed.* **2012**, *51*, 8356 – 8360; *Angew. Chem.* **2012**, *124*, 8481 – 8485.
[31] T. Nuida, T. Matsuda, H. Tokoro, S. Sakurai, K. Hashimoto, S. Ohkoshi, *J. Am. Chem. Soc.* **2005**, *127*, 11604 – 11605.
[32] C. Train, T. Nuida, R. Gheorghe, M. Gruselle, S. Ohkoshi, *J. Am. Chem. Soc.* **2009**, *131*, 16838 – 16843.
[33] E. E. Moushi, C. Lampropoulos, W. Wernsdorfer, V. Nastopoulos, G. Christou, A. Tasiopoulos, *J. Am. Chem. Soc.* **2010**, *132*, 16146 – 16155.
[34] Y.-Z. Zheng, M. Evangelisti, R. E. P. Winpenny, *Angew. Chem. Int. Ed.* **2011**, *50*, 3692 – 3695; *Angew. Chem.* **2011**, *123*, 3776 – 3779.
[35] D. Pinkowicz, R. Podgajny, B. Nowicka, S. Chorazy, M. Reczyński, B. Sieklucka, *Inorg. Chem. Front.* **2015**, *2*, 10 – 27.
[36] Z. J. Zhong, H. Seino, Y. Mizobe, M. Hidai, A. Fujishima, S. Ohkoshi, K. Hashimoto, *J. Am. Chem. Soc.* **2000**, *122*, 2952 – 2953.
[37] J. Larionova, M. Gross, M. Pilkington, H. Andres, H. Stoeckli-Evans, H. U. Güdel, S. Decurtins, *Angew. Chem. Int. Ed.* **2000**, *39*, 1605 – 1608; *Angew. Chem.* **2000**, *112*, 1667 – 1672.
[38] F. Bonadio, M. Gross, H. Stoeckli-Evans, S. Decurtins, *Inorg. Chem.* **2002**, *41*, 5891 – 5896.
[39] Y. Song, P. Zhang, X.-M. Ren, X.-F. Shen, Y.-Z. Li, X.-Z. You, *J. Am. Chem. Soc.* **2005**, *127*, 3708 – 3709.
[40] M. G. Hilfiger, H. Zhao, A. Prosvirin, W. Wernsdorfer, K. R. Dunbar, *Dalton Trans.* **2009**, 5155 – 5163.
[41] S. Chorazy, R. Podgajny, W. Nogas, W. Nitek, M. Kozieł, M. Rams, E. Juszynska-Galazka, J. Zukrowski, C. Kapusta, K. Nakabayashi, T. Fujimoto, S. Ohkoshi, B. Sieklucka, *Chem. Commun.* **2014**, *50*, 3484 – 3487.
[42] R. Podgajny, S. Chorazy, W. Nitek, M. Rams, A. M. Majcher, B. Marszałek, J. Żukrowski, C. Kapusta, B. Sieklucka, *Angew. Chem. Int. Ed.* **2013**, *52*, 896 – 900; *Angew. Chem.* **2013**, *125*, 930 – 934.
[43] P. Gütlich, A. B. Gaspar, Y. Garcia, *Beilstein J. Org. Chem.* **2013**, *9*, 342 – 391.
[44] C. Chong, H. Mishra, K. Boukheddaden, S. Denise, G. Bouchez, E. Collet, J.-C. Ameline, A.-D. Naik, Y. Garcia, F. Varret, *J. Phys. Chem. B* **2010**, *114*, 1975 – 1984.
[45] A. Galet, A. B. Gaspar, M. C. Muñoz, G. V. Bukin, G. Levchenko, J. A. Real, *Adv. Mater.* **2005**, *17*, 2949 – 2953.
[46] C. Lochenie, W. Bauer, A. P. Railliet, S. Schlamp, Y. Garcia, B. Weber, *Inorg. Chem.* **2014**, *53*, 11563 – 11572.
[47] A. B. Gaspar, M. C. Muñoz, J. A. Real, *J. Mater. Chem.* **2006**, *16*, 2522 – 2533.
[48] B. Schneider, S. Demeshko, S. Dechert, F. Meyer, *Angew. Chem. Int. Ed.* **2010**, *49*, 9274 – 9277; *Angew. Chem.* **2010**, *122*, 9461 – 9464.
[49] R.-J. Wei, Q. Huo, J. Tao, R.-B. Huang, L.-S. Zheng, *Angew. Chem. Int. Ed.* **2011**, *50*, 8940 – 8943; *Angew. Chem.* **2011**, *123*, 9102 – 9105.
[50] T. Matsumoto, G. N. Newton, T. Shiga, S. Hayami, Y. Matsui, H. Okamoto, R. Kumai, Y. Murakami, H. Oshio, *Nat. Commun.* **2014**, *5*, 3865.
[51] M. Shatruk, A. Dragulescu-Andrasi, K. E. Chambers, S. A. Stoian, E. L. Bominaar, C. Achim, K. R. Dunbar, *J. Am. Chem. Soc.* **2007**, *129*, 6104 – 6116.
[52] R. Boča, I. Šalitroš, J. Kožíšek, J. Linares, J. Moncoľ, F. Renz, *Dalton Trans.* **2010**, *39*, 2198 – 2200.
[53] M. B. Duriska, S. M. Neville, B. Moubaraki, J. D. Cashion, G. J. Halder, K. W. Chapman, C. Balde, J. F. Letard, K. S. Murray, C. Kepert, S. R. Batten, *Angew. Chem. Int. Ed.* **2009**, *48*, 2549 – 2552; *Angew. Chem.* **2009**, *121*, 2587 – 2590.

[54] F. Renz, D. Hill, M. Klein, J. Hefner, *Polyhedron* **2007**, *26*, 2325 – 2329.
[55] F. Renz, S. Jung, M. Klein, M. Menzel, A. F. Thünemann, *Polyhedron* **2009**, *28*, 1818 – 1821.
[56] M. V. Bennett, J. R. Long, *J. Am. Chem. Soc.* **2003**, *125*, 2394 – 2395.
[57] D. E. Freedmann, M. V. Bennett, J. R. Long, *Dalton Trans.* **2006**, 2829 – 2834.
[58] W. Kosaka, K. Nomura, K. Hashimoto, S. Ohkoshi, *J. Am. Chem. Soc.* **2005**, *127*, 8590 – 8591.
[59] R. Podgajny, S. Chorazy, W. Nitek, M. Rams, M. Bałanda, B. Sieklucka, *Cryst. Growth Des.* **2010**, *10*, 4693 – 4696.
[60] CCDC-1039292 ($\mathbf{1}^{HT}$) and 1039293 ($\mathbf{1}^{LT}$) contain the supplementary crystallographic data for this paper. These data can be obtained free of charge from The Cambridge Crystallographic Data Centre via www.ccdc.cam.ac.uk/data_request/cif.

Received: January 13, 2015
Published online: March 3, 2015

